NeuroImage 340 (2026) 122211

Contents lists available at ScienceDirect

NeuroImage

journal homepage: www.elsevier.com/locate/ynimg

Task-based functional connectivity is sufficient to capture individual differences in functional selectivity across multiple cortical systems

Isaac Liao [a,*], Zeynep M. Saygin [a], Keara M. Ginell [a], Kendrick N. Kay [b], David E. Osher [a]

[a] Department of Psychology, The Ohio State University, Columbus, Ohio, USA
[b] Department of Radiology, University of Minnesota, Minneapolis, Minnesota, USA

ARTICLE INFO

Keywords:
Functional connectivity
Resting-state
Task fMRI
Connectivity fingerprinting

ABSTRACT

Most studies of brain networks use resting-state fMRI to characterize the brain's intrinsic functional organization. However, recent work has questioned whether we should rely exclusively on resting-state data to define this organization. Using a connectivity fingerprint modeling framework, we test whether functional connectivity estimated from task fMRI data can predict task selectivity in visual, language, and spatial working memory tasks, at the individual subject level. We find that connectivity derived from these task contexts predicts responses comparably to connectivity derived from resting-state data. This pattern held across the three controlled cognitive localizers acquired within the same preprocessing framework. These findings suggest that task fMRI can capture fine-grained individual differences in brain network architecture that are comparable to those captured at rest, broadening the potential utility of task data for investigating functional organization of brain networks.

1. Introduction

Currently, most studies in network neuroscience collect structural imaging and resting-state fMRI, which measures spontaneous brain activity in the absence of explicit task or external stimuli. Resting-state scans are typically used to estimate functional connectivity (FC), defined as the temporal co-fluctuation of activity between brain regions (Biswal et al., 1995; Fox and Raichle, 2007). Because these spontaneous correlations are measured during an unconstrained, "passive" state, resting-state FC is thought to reflect the brain's intrinsic functional organization (Dosenbach et al., 2007; Kelly et al., 2008). Resting-state FC has become a central tool in network neuroscience because it captures distributed patterns of interaction across the brain, providing insights beyond localized activation measures derived from traditional task-based analyses. This is evidenced by the fact that FC is widely used to elucidate brain-brain relationships (Cole et al., 2016; Hiersche et al., 2025; Molloy et al., 2024; Ngo et al., 2022; Tavor et al., 2016; Zheng et al., 2022) as well as brain-behavior relationships (Finn and Bandettini, 2021; Wei et al., 2024). However, FC can also be computed using task-based fMRI (Fair et al., 2007), and it is currently being debated whether resting-state fMRI is necessary in the field of network neuroscience (Finn, 2021).

Importantly, resting-state FC is highly reliable across sessions, making it a stable neural signature suitable for longitudinal and cross-sectional studies (Gratton et al., 2018a). These connectivity patterns can predict both state-like and trait-like differences across individuals, including attention (Song and Rosenberg, 2021), age (Dosenbach et al., 2010; Nielsen et al., 2019), personality (Dubois et al., 2018; Hsu et al., 2018), lifestyle factors (Smith et al., 2015), symptoms of autism and attention-deficit disorder (Lake et al., 2019), and is characteristic enough to identify individuals (Finn et al., 2015a). FC has also been applied to estimate developmental (Yin et al., 2025) and aging (Farràs-Permanyer et al., 2019) trajectories and identify biomarkers of disease (Hua et al., 2023). Beyond predicting behavioral and clinical traits, FC can also predict task-evoked brain responses at the level of individual subjects across a wide range of cognitive domains (Cole et al., 2016; DiNicola et al., 2020; Du et al., 2025; Hiersche et al., 2025; Molloy et al., 2024; Ngo et al., 2022; Tavor et al., 2016; Zheng et al., 2022). This ability to predict activation patterns from intrinsic connectivity is theoretically important because it suggests that large-scale network architecture constrains how task-related information flows through the brain. In this framework, task-evoked responses emerge from distributed patterns of connectivity, and the predictive models provide estimates of the importance of connections between brain regions for functional

* Corresponding author.
E-mail address: liao.798@osu.edu (I. Liao).

https://doi.org/10.1016/j.neuroimage.2026.122211
Received 28 May 2026; Received in revised form 4 September 2026; Accepted 8 September 2026
Available online 9 September 2026
1053-8119/© 2026 The Authors. Published by Elsevier Inc. This is an open access article under the CC BY-NC license (http://creativecommons.org/licenses/by-nc/4.0/).

response (i.e. a connectivity fingerprint for a given functional region, Mahon and Caramazza, 2011; Mars et al., 2018; Osher et al., 2016; Passingham et al., 2002; Tobyne et al., 2018).

Predicted task activation maps also have important practical applications. They can localize functional regions in the absence of dedicated localizer tasks (Molloy et al., 2024) and estimate task responses in populations where collecting high-quality task fMRI data is difficult, such as children or clinical populations (Parker Jones et al., 2016; Tik et al., 2021). Prior work has shown, for example, that connectivity patterns can predict the location of the visual word form area before literacy develops (Li et al., 2020) and can identify the fusiform face area in congenitally blind individuals (Ratan Murty et al., 2020). Together, these findings suggest that predicted activation maps can serve as individualized neural signatures for studying cognition, development, and clinical variability.

Most prior work predicting task responses has relied on resting-state FC, based on the assumption that resting activity provides a task-independent estimate of intrinsic functional organization. However, there is growing debate over whether resting-state fMRI is uniquely necessary for studying brain networks (Finn, 2021). Although rest is often treated as a passive baseline, resting-state activity itself may reflect ongoing cognitive processes that can vary across individuals and sessions (Buckner et al., 2013; Morcom and Fletcher, 2007). At the same time, FC can also be reliably estimated during tasks (Fair et al., 2007), and recent work suggests that task-derived FC may better predict behavior than resting-state FC in some contexts (Greene et al., 2018, 2020; Jiang et al., 2020; Sripada et al., 2020)—for example, task-based connectivity has been shown to outperform resting-state connectivity in predicting general cognitive ability (Sripada et al., 2020), consistent with the broader idea that engaging the brain in an active state may better reveal aspects of its functional architecture. A parallel line of work using naturalistic paradigms has reached similar conclusions: movie-watching connectivity has been shown to outperform resting-state connectivity both in predicting task-evoked activation patterns and downstream behavioral measures (Finn and Bandettini, 2021; Gal et al., 2022; see Bernstein-Eliav and Tavor, 2024 for a review). Furthermore, connectivity-based parcellations derived from residualized task and resting-state data are highly similar (Du et al., 2025), suggesting that task-based FC may capture much of the same large-scale functional architecture traditionally attributed to rest. Consistent with this idea, previous studies have reported substantial similarity between correlation patterns obtained from residualized task and resting-state data (Cho et al., 2021; Elliott et al., 2019; Fair et al., 2007; Gratton et al., 2018a; Kraus et al., 2021). However, studies examining individual differences have also shown that portions of FC are sensitive to task states (Geerligs et al., 2015; Salehi et al., 2020), indicating that task engagement may introduce meaningful state-dependent information. Thus, although task FC appears broadly similar to resting-state FC at the group and network levels, it remains unclear whether the shared connectivity structure is sufficient to capture fine-grained individual differences in voxelwise task-evoked responses. This question also has important practical implications. Because many fMRI experiments already include task scans, leveraging these data to analyze brain networks could reduce the need for additional resting-state acquisitions.

Here, using a connectivity fingerprint modeling framework, we test whether FC derived from task fMRI can predict responses in other, distinct tasks, and whether such predictions perform as well as or better than those derived from resting-state data. Specifically, we ask whether a model trained on FC estimates from one task can generalize to predict task selectivity in different cognitive domains, and whether these predictions remain precise for functional regions of interest within each network. While previous work has shown that structural and resting-state connectivity can predict task selectivity in high-level visual regions at the individual-subject level (Molloy et al., 2024; Osher et al., 2016, 2019; Saygin et al., 2012; Tavor et al., 2016), it remains unclear whether task-based connectivity from an unrelated task domain can a) predict responses to higher-level cognitive tasks such as working memory or language processing and b) do so in a selective manner. Our results show that task-derived connectivity is as effective as, and in some cases superior to, resting-state connectivity for predicting task-evoked functional regions across multiple cognitive domains, including predictions across highly disparate tasks (e.g., visual task-derived FC predicting auditory language fROIs and their hemispheric laterality).

2. Methods

2.1. Participants

A total of 48 participants (aged 18 to 55; mean = 24.4 yr, SD = 6.3 yr; 21 male) recruited at The Ohio State University were included in the study. There were 35 within-sample participants (aged 18 to 55; mean = 24.7 yr, SD = 7 yr; 13 male) who participated in all tasks and whose connectivity data were used to train the predictive models. The other 13 individuals (aged 18 to 30; mean = 23.4 yr, SD = 3.6 yr; 8 male) participated in only the dynamic visual localizer and spatial working memory tasks, and their data were used to further validate the models as an out-of-sample dataset. The study was approved by the Institutional Review Board at The Ohio State University, informed consent was obtained from all participants, and the study was conducted following all relevant guidelines and regulations.

2.2. fMRI tasks

To obtain responses of functional regions of interest (fROIs) involved in high-level vision, language, and spatial working memory tasks, we used three independent functional localizers: a dynamic visual localizer (Julian et al., 2012), an auditory language localizer (Fedorenko et al., 2010), and a spatial working memory task commonly used to evoke responses in the multiple-demand (MD) network (Fedorenko et al., 2013).

2.2.1. *Dynamic visual localizer* (*Julian et al., 2012*)

Participants viewed a series of 3 s video clips in color. Each video clip contained moving stimuli from one of five categories: faces, bodies (without faces), objects, scenes, and scrambled objects. Participants were asked to press a button whenever they saw a repeating stimulus (1-back). Stimuli were presented in a block design, and each block contained 6 videos from the same category (18 s total), with two blocks per category per run, arranged in a palindromic sequence and interleaved with three fixation blocks. Condition order was randomized across participants.

2.2.2. *Auditory language localizer* (*Fedorenko et al., 2010*)

Participants listened to blocks of meaningful sentences, nonsense sentences composed of phonemically intact but meaningless words (controlling for prosody), and texturized speech (controlling for low-level acoustic properties). Each run consisted of four blocks of each condition and three fixation blocks (14 s). Blocks were 18 s long and comprised three 6-s trials, each ending with a visual cue prompting a button press.

2.2.3. *Spatial working memory (SWM) task* (*Fedorenko et al., 2013*)

This task contrasted easy and hard conditions to vary cognitive load, engaging the domain-general multiple-demand network. In the easy condition, three individual squares within a 12-square grid flashed blue sequentially, and participants were asked to remember which squares had been colored. In the hard condition, three pairs of squares flashed sequentially, increasing memory demands. After viewing the sequence, participants selected between two test grids—one matching and one mismatching the sequence—via button press. Each run included three sets of two blocks per condition (28 s each), separated by 16-s fixation

periods. The order of easy and hard blocks was randomized across participants.

2.3. MRI data acquisition

All MRI data were collected on a Siemens Prisma 3T scanner at The Ohio State University using a 32-channel head coil. Each participant completed a high-resolution structural scan, two runs of each functional localizer task, and one resting-state run. The order of the resting-state and functional localizer scans were randomized across participants. The whole-brain T1-weighted anatomical images were acquired with an gradient echo (MPRAGE) sequence (repetition time (TR) = 2300 ms, echo time (TE) = 2.9 ms, voxel size = 1.0 mm^3). All functional and resting-state scans were obtained with echo-planar imaging (EPI) sequence for whole-brain coverage (TR = 1000 ms, TE = 28 ms, voxel size = 2 × 2 × 3 mm^3, 120 × 120 in-plane resolution, 56 slices). The number of volumes per run was 234 for the dynamic visual localizer, 244 for the auditory language localizer, 400 for the spatial working memory task, and 580 for the resting-state scan.

2.4. Preprocessing

All structural data were preprocessed using Freesurfer's recon-all pipeline (Dale et al., 1999) with default parameter values. Major preprocessing steps include intensity correction, skull stripping, surface co-registration, surface-smoothing (3 mm FWHM), white matter and subcortical segmentation, and cortical parcellation.

Resting-state data were preprocessed using FsFast (Fischl, 2012). Data were motion corrected, surface-registered, surface-smoothed with a 4 mm FWHM kernel, and denoised with aCompCor (Behzadi et al., 2007) using 5 principal components each from white matter and cerebrospinal fluid. Time points with framewise displacement greater than 0.5 mm were excluded from the analysis.

All task data were motion corrected, distortion corrected, and surface-smoothed with a 4 mm FWHM kernel. These data were then fit with a general linear model (GLM) against task-based regressors which were convolved with a canonical gamma hemodynamic response function, as well as the movement parameters estimated during motion correction. The GLM coefficients were further analyzed to measure voxelwise constrast t-values, and the residuals of the GLMs were then further denoised with aCompCor as above, and high motion datapoints were excluded. Condition-specific contrasts were defined as follows. For the dynamic visual localizer, contrasts included Faces > All others, Bodies > All other, Objects > All others, and Scenes > All others. For the auditory language localizer, we contrasted Sentences > Nonsense. For the spatial working memory task, we contrasted the Hard > Easy conditions. The resulting contrast significance maps and β estimates were projected into fsaverage space and used for the following modeling and analysis.

2.5. Estimation of functional connectivity matrices

Both resting-state and task data were used to estimate functional connectivity. Throughout this manuscript, "task-derived FC" and "task connectivity" refer to functional connectivity estimated from task fMRI time series after GLM-based residualization of task-evoked activity, unless otherwise specified. This residualized task FC is therefore best understood as reflecting residual covariance among vertices after task-locked variance has been removed, rather than task-evoked coactivation. To evaluate the contribution of this residualization step, we additionally computed FC directly from non-residualized task time series and repeated our full modeling pipeline (see Methods 2.6) using this task FC. Results using non-residualized task FC were similar to those obtained using residualized task FC (see Supplementary Fig. S2). We used "task-based connectivity" to refer to both residualized and non-residualized FC generally.

Matrices of FC were defined for each visual, language, and spatial working memory fROI search space from Julian et al. (2012), Fedorenko et al. (2010), and Fedorenko et al. (2013), respectively. In these studies, the fROI search spaces were defined using the Group-Constrained Subject-Specific (GSS) method designed to discover parcels that are activated most systematically across subjects for the contrasts of interest (Julian et al., 2012). These search spaces are thus larger than an individual subject's actual fROIs and are ideal for modelling the space around known ROIs while remaining blinded to the actual responses of each individual. For visual regions, we included 10 bilateral fROIs (20 total): 3 face regions (FFA: fusiform face area, OFA: occipital face area, STS: superior temporal sulcus), 2 body region (EBA: extrastriate body area, FBA: fusiform body area), 2 object regions (LO: lateral occipital, PFS: posterior fusiform sulcus), and 3 scene regions (PPA: parahippocampal place area, RSC: retrosplenial cortex, TOS: transverse occipital sulcus). For language regions, we included 6 bilateral fROIs (12 total): anterior temporal lobe (ATL), inferior frontal gyrus (IFG), orbital inferior frontal gyrus (IFGorb), middle frontal gyrus (MFG), middle temporal lobe (MTL), and posterior temporal lobe (PTL). For spatial working memory regions, we included 10 bilateral fROIs (20 total): anterior precentral gyrus (PrecG), opercular part of inferior frontal gyrus (IFGop), anterior parietal cortex, insula, medial frontal cortex (MFC), middle frontal gyrus (MFG), orbital middle frontal gyrus (MFGorb), middle parietal cortex, posterior parietal cortex (PPC), and superior frontal gyrus (SFG).

For each fROI search space, FC was computed as the Fisher-transformed Pearson correlation between the time series of every vertex within the fROI search space and the mean time series of each Glasser multimodal parcel in the same hemisphere (179 parcels total). This procedure generated four connectivity matrices with dimensions corresponding to the number of vertices in the fROI search space by 179 parcels. Computing FC at the vertex level preserved fine-grained spatial variation in connectivity patterns, allowing the models to make vertexwise predictions of task selectivity within each fROI search space. Connectivity estimates were restricted to ipsilateral parcels primarily to reduce model dimensionality and mitigate overfitting while retaining the majority of relevant large-scale connectivity structure.

2.6. Predictive model training and application

For a given fROI search space (a larger space around the actual fROI), connectivity fingerprint models were designed using $\mathscr{L}_2$-regularized linear models (also known as ridge regression) to predict an individual's task contrast (t-values) using that individual's functional connectivity as regressors. Models were trained to only predict the task selectivity relevant to each fROI. Visual fROI models were trained using visual contrasts, language fROI models were trained using the Sentences > Nonsense contrast, and spatial working memory (SWM) fROI models were trained using the Hard > Easy contrast. Cross-domain contrasts (e.g., training visual fROIs using language contrast) were not used. The regression coefficients were a vector of length p, the number of parcels ipsilateral to the fROI search space (179 parcels). The model predictions of a subject's task selectivity within the fROI search space were a vector of length v, the number of vertices in the search space. The predictions were obtained by computing the dot product between a subject's connectivity matrix (i.e., vertices by 179 parcels) and the model coefficients. We designed four final models for each fROI search space using four different types of FC (4 × 52 = 208 models total).

The model training approach has previously been described in Osher et al., 2019 and Molloy et al., 2024 (see Fig. 1). We used a sample of 35 subjects to train the models. Briefly, for each fROI search space, the λ parameter for an $\mathscr{L}_2$-regularized linear model was optimized through an inner-loop leave-one-subject-out cross validation, where 100 candidate λ values logarithmically spaced between 10^{-5} and 10^{2} were fit, and the best fitting model (by mean squared error), averaged across left out subjects, was identified. Models were trained separately for each type of

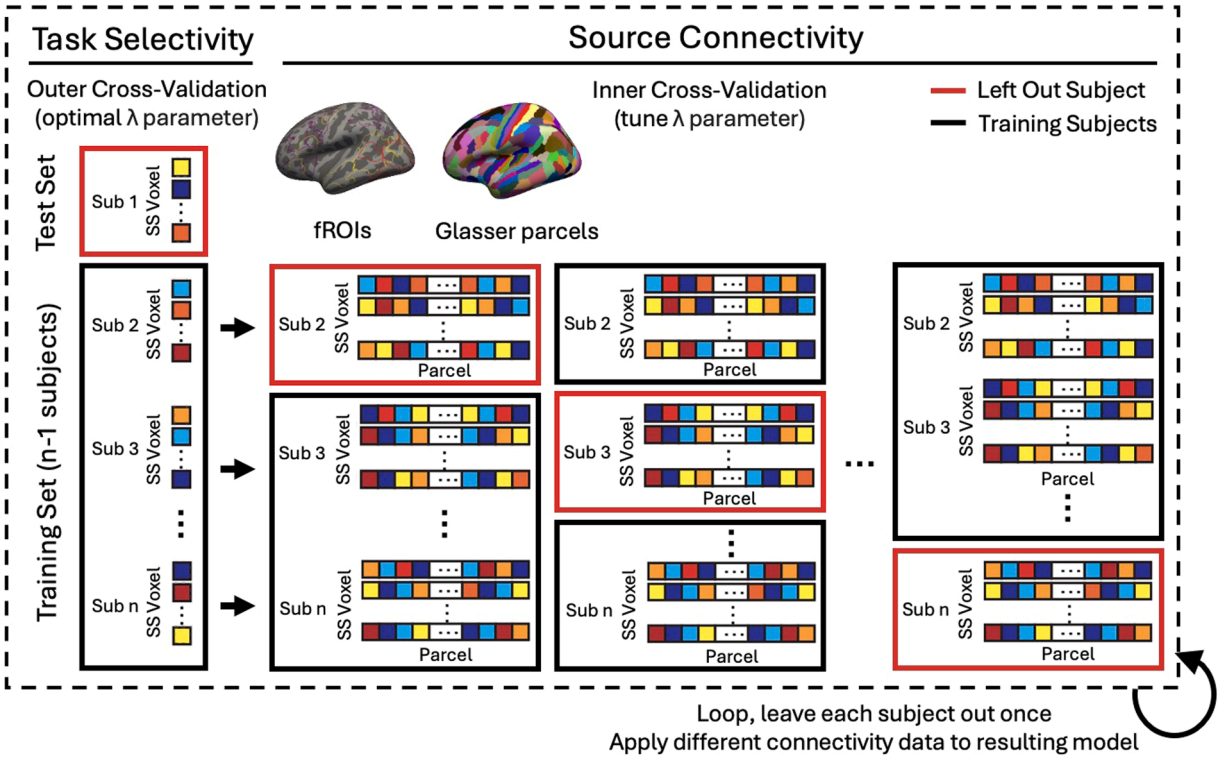

Fig. 1. Model training and application schematic. For each fROI search space (a larger space around the actual fROI, abbreviated as SS in the figure), a model was trained separately with each type of FC to predict an individual's task selectivity (each search space voxel's t-statistic for the appropriate contrast) using that same individual's resting-state or task-derived FC (each search space voxel's connectivity to each Glasser parcel). A nested cross validation approach was adopted to optimize the model's regularization parameter (λ for $\mathscr{l}_2$-regularized linear models).

FC (referred to as "source connectivity") and then used to predict neural responses using different types of FC (referred to as "applied connectivity") for the left-out subject in the outer-loop "cross validation", using that same subject's data (Table 1). To avoid circularity between the connectivity used to generate predictions and the task selectivity being predicted, source and applied connectivity for each fROI's prediction was always derived from a task other than the one defining that fROI's selectivity (e.g., language- or SWM-derived FC was used to predict visual category selectivity, and vice versa). Same-task FC was therefore never used to predict selectivity within its own domain in the comparisons reported in Figs. 2 and 3. The results of this within-sample model application were almost perfectly replicated with an independent, out-of-sample dataset of 13 participants which used no cross-validation. For these participants, models were designed as described above, except that no subject was left out in the outer-loop; instead, FC and BOLD data from the 35 participants above were used for model training (resulting in a small 2.86% increase in training data). These trained models were then applied to FC data from a completely independent set of participants, whose data were not part of the modeling procedure and were left out of all analyses until all other experiments and analyses had been completed (Table 1). Prediction accuracy was quantified as the mean Pearson correlation between predicted and observed task selectivity across subjects. These values were Fisher-transformed prior to averaging, and then transformed back to [−1 1].

As a baseline for model performance, empirical chance levels were estimated using a permutation procedure in which task selectivity values were randomly shuffled across subjects prior to model training. Models were then trained on the permuted data and evaluated on left-out subjects using the same cross-validation procedure as the true models. This approach preserves the overall distribution of task selectivity values while disrupting their correspondence with functional connectivity, providing an estimate of the prediction accuracy expected by chance in the absence of a true relationship between functional connectivity and task selectivity. The empirical chance levels are plotted in Figs. 2 and 4.

To evaluate whether functional connectivity provides predictive

Table 1
Train/test structure for within-sample and out-of-sample connectivity fingerprint models.

Analysis	Subjects	Training data (model fitting)	FC used at application (generates prediction)	Evaluation target (observed contrast)
Within-sample (nested leave-one-subject-out)	N = 35; each subject held out in turn	Remaining 34 subjects' *source connectivity*, paired with their own observed contrast for the domain being predicted	Held-out subject's *applied connectivity*	Held-out subject's own observed contrast for the domain being predicted
Out-of-sample validation	N = 35 (train) → N = 13 independent subjects (test)	All 35 subjects' *source connectivity*, paired with their own observed contrast for the domain being predicted	Each of the 13 independent subjects' *applied connectivity*	Each of the 13 independent subjects' own observed contrast for the domain being predicted

Note. "Source connectivity" refers to the functional connectivity (FC) type—resting-state or one of the task conditions—used for model fitting. "Applied connectivity" refers to the FC type from the subject(s) being predicted, to which the model is applied to generate a predicted activation map. Source and applied FC type were independently varied across all combinations of rest and the two non-target-domain task types for each domain (yielding a 3 × 3 design per domain); this table describes the general train/test procedure common to all such combinations.

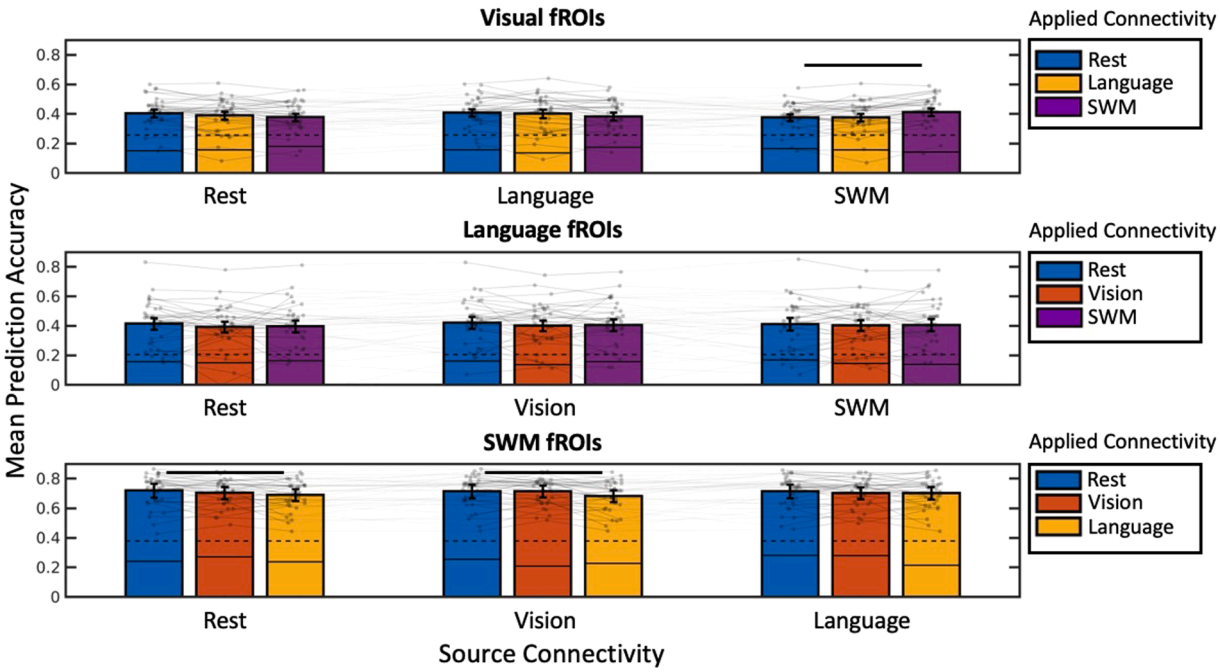

Fig. 2. Prediction accuracy for each combination of source connectivity and applied connectivity. Each row shows mean prediction accuracy (Pearson's r) across within-sample participants for fROIs within each domain. Bars are grouped by source connectivity—i.e., the connectivity type that was used to build the model. Each bar within a group represents the accuracy of applied connectivity—i.e., the connectivity type the model was applied to. FC from the same task were never used to predict selectivity within their own domain. The solid horizontal line within each bar indicates the empirical chance level (i.e., prediction accuracy expected by chance in the absence of a true relationship between functional connectivity and task selectivity) associated with each source-applied connectivity combination. The dashed horizontal line within each bar indicates the spatial baseline model for that condition (i.e., prediction accuracy based solely on each subject's native vertex coordinates, without functional connectivity information). Error bars reflect the standard errors of the means. Horizontal lines indicate a significant difference in mean prediction accuracy between models (paired *t*-tests, Holm-Bonferroni corrected for 18 comparisons, $p < 0.05$). In almost all cases, the accuracy of models either built by or applied to resting-state connectivity are not significantly different from task-derived connectivity.

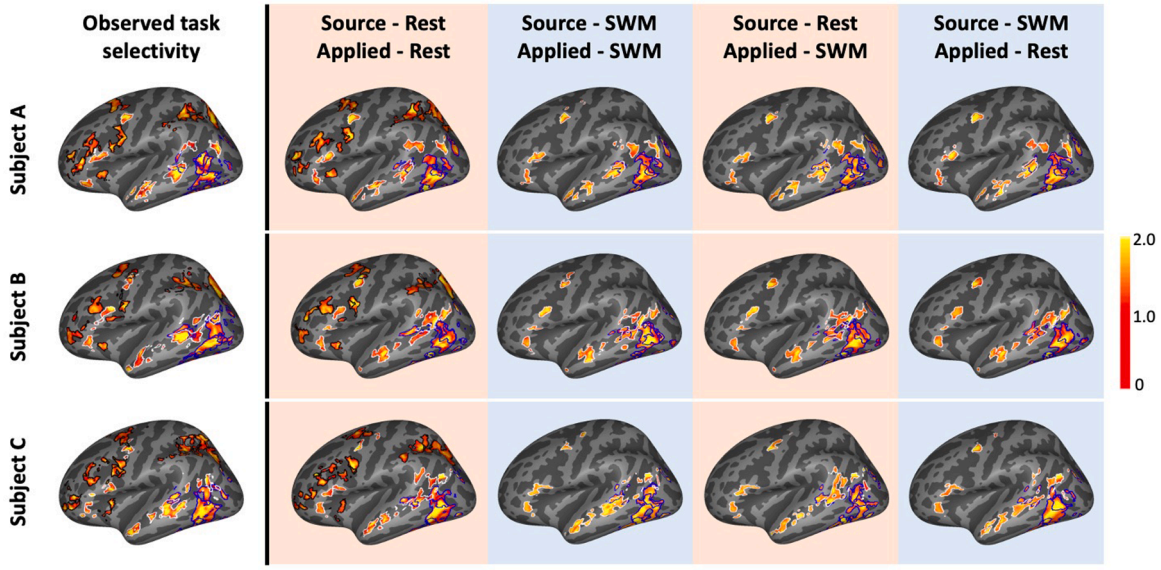

Fig. 3. Predicted and observed task selectivity maps for three subjects. The left panel displays the observed task selectivity for all left hemisphere fROIs, the colored panels display the predicted patterns of selectivity for each combination of source and applied connectivity from resting-state and SWM task data. FC from the same task were never used to predict selectivity within their own domain (see methods), and so frontal and parietal SWM fROIs are not included in the final 3 columns. Regions outlined in blue denote visual fROIs, regions outlined in white denote language fROIs, and regions outlined in black denote SWM fROIs. Regardless of source or applied connectivity type, the selectivity predictions are highly similar to each other and to the observed selectivity. Units are z-scores.

information beyond simple anatomical position, we additionally implemented a spatial baseline model, which was designed identically to the connectivity-based models, except that the covariates were the x, y, and z coordinates of each subject's native pial surface projected onto fsaverage, for a given search space. Because these coordinates were not derived from a group-level template but retain subject-specific anatomical variation, this baseline can capture both predictable spatial regularities in task selectivity (e.g., its typical location within a

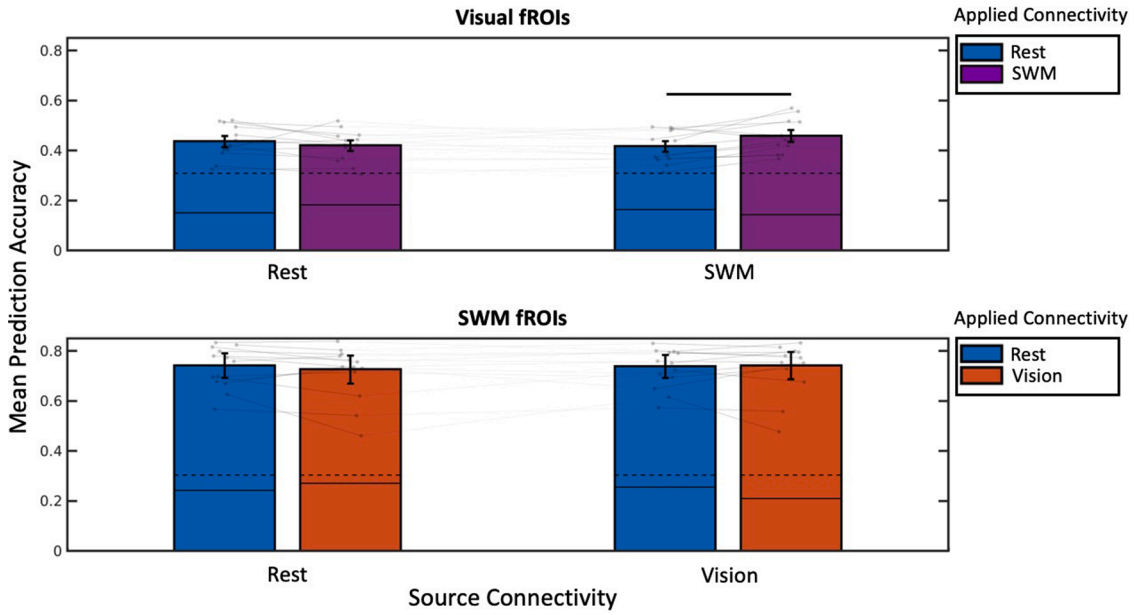

Fig. 4. Prediction accuracy of out-of-sample participants for each combination of source connectivity and applied connectivity. Each row shows mean prediction accuracy (Pearson's r) across out-of-sample participants for fROIs within each domain. Bars are grouped by source connectivity and each bar within a group represents the accuracy of applied connectivity. The solid horizontal line within each bar indicate the empirical chance level (i.e., prediction accuracy expected by chance in the absence of a true relationship between functional connectivity and task selectivity) associated with each source-applied connectivity combination. The dashed horizontal line within each bar indicates the spatial baseline model for that condition (i.e., prediction accuracy based solely on each subject's native vertex coordinates, without functional connectivity information). Error bars reflect the standard errors of the means. The significance line indicates a significant difference in mean prediction accuracy between models applied to rest and those applied to task (paired *t*-tests, Holm-Bonferroni corrected across 4 comparisons, $p < 0.05$). Note that the 13 out-of-sample subjects did not complete the language task, so language fROIs are not included in the comparisons. Again, as in Fig. 2, in all but one case, the accuracy of models either built by or applied to resting-state connectivity are not significantly different from task-derived connectivity.

search space) and idiosyncratic individual differences in anatomy. This baseline model was trained and evaluated using the same nested leave-one-subject-out cross-validation procedure as our connectivity fingerprinting models, allowing direct comparison of prediction accuracy between models based on functional connectivity and models based solely on anatomical position. The prediction accuracies from these models are plotted in Fig. 2 as dashed lines.

3. Results

3.1. Task-based connectivity from diverse task localizers predicts individual's fROIs as well as resting-state connectivity

To determine whether FC estimates from one task can generalize to predict task selectivity in other tasks and how its performance compares to resting-state FC, we first built a connectivity fingerprint model from each FC type (referred to as "source connectivity", the type of FC used to build the model) and applied them to either the same or different FC types (referred to as "applied connectivity", the type of FC that the model is applied to in order to predict neural responses). For example, we built a model to predict each visual fROI from resting-state as source connectivity, and then applied it to the FC derived from the residuals of the spatial working memory (SWM) task, the applied connectivity. Overall prediction accuracy was high across all fROIs and models (grand mean r = 0.47, SD = 0.31), exceeding empirical chance levels (Pearson's r between 0.2 and 0.3) by more than two-fold and closely matching observed patterns of task selectivity (Fig. 2, solid line in each bar). Accuracies were also significantly higher for all connectivity fingerprint models than for the spatial baseline models (paired *t*-tests, Holm-Bonferroni corrected for 27 comparisons, all $p < 0.05$), in which prediction relied solely on each subject's native vertex coordinates, indicating that functional connectivity captures predictive information beyond subjects' anatomical positions alone (Fig. 2, dashed line in each bar). Beyond prediction accuracy, all models captured individual differences in task selectivity (Fig. 3): each subject's predicted activation map was more similar to their own actual map than to those of any other subject in the sample (Kolmogorov-Smirnov tests between self vs. other distributions, all $p < 10^{-8}$) (see supplementary Fig. S1). This self-specificity was not simply attributable to subjects' anatomy: the spatial baseline models showed no significant self-vs-other specificity (Kolmogorov-Smirnov tests, all $p > 0.05$), indicating that connectivity-derived predictions capture subject-specific neural response patterns beyond what anatomical position alone can explain.

To test whether prediction accuracy depended on the type of connectivity used to build or apply the model, we ran a two-way 3 × 3 repeated-measures ANOVA for each fROI domain, with source connectivity and applied connectivity as within-subject factors, each with three levels (rest and two task FC types, Supplementary Table S1). This allowed us to determine whether models built from or applied to task-derived FC performed comparably to those built from or applied to resting-state FC, both independently and in combination. For each domain tested, there was no main effect of source or applied connectivity ($p > 0.05$): models fit equally well regardless of whether they were built from, or applied to, rest- or task-derived FC. Significant interactions were observed for the visual ($F(4, 136) = 25.94$, $p < 0.001$) and SWM tasks ($F(4, 136) = 21.77$, $p < 0.001$). To follow up on these interactions, we conducted post hoc paired *t*-tests comparing prediction accuracy between each task-based source-applied combination and the corresponding rest-applied combination, with accuracies first averaged across fROIs within each domain for each subject. Within each domain, p-values from these post hoc tests were Holm-Bonferroni corrected across the 18 pairwise comparisons tested. These post hoc comparisons revealed that these interactions were driven by modestly divergent accuracies in all cases. In visual fROIs, the significant interaction occurred when SWM was the source connectivity and applied to SWM connectivity, compared to when it was applied to rest (Δprediction

accuracy = 0.035, t(34) = −3.91, p = 0.0076, Holm-Bonferroni corrected for 18 comparisons). In SWM fROIs, the significant interaction occurred when the source was either rest or vision, and applied to language, compared to when it was applied to rest (Δprediction accuracy = −0.024, t(34) = 2.93, p = 0.036, and Δprediction accuracy = −0.025, t(34) = 2.96, p = 0.036, respectively; Holm-Bonferroni corrected p values across 18 comparisons), see Fig. 2. Thus, in all but a handful of cases, the accuracies of models either built by or applied to resting-state connectivity are not significantly different from task-derived connectivity. Taken together, these results indicate that task-derived connectivity, across the three localizers tested here, predicts individual task selectivity as well as resting-state connectivity, even when the connectivity used to build the model was derived from a task other than the one whose selectivity was being predicted.

3.2. Out-of-sample data is well predicted by resting-state and task-derived connectivity

We next applied the models built from within-sample subjects to an additional 13 out-of-sample subjects who did not complete all three tasks. This allows us to determine whether the high prediction accuracies we observed were due to overfitting. The overall accuracy is high (grand mean r = 0.57, SD = 0.26) (Fig. 4), and in all cases higher than the accuracy observed with within-sample participants (Welch's t-test of out-of-sample vs. within-sample accuracies, t(7011) = 22.52, $p < 0.001$). This shows that the models likely did not overfit the data and are generalizable. In addition, a similar pattern was observed as the training participants, where the type of source or applied connectivity does not appreciably influence predictions of task selectivity in visual and spatial working memory regions (Fig. 2). Together, these results confirmed that task selectivity at the level of individual subject fROIs can be predicted by task-derived connectivity, regardless of task type, and that this is the case even when the source connectivity does not match applied connectivity.

3.3. Laterality in task activation predicted by task-derived connectivity

Our results above revealed that task responses within individual subject visual, language, and SWM fROIs can be predicted from independent task-derived connectivity (Figs. 2 and 3), with the SWM fROIs achieving remarkable accuracies around r = 0.7, similar to that reported in Osher et al. (2019) for the related dorsal attention network. The same fMRI data can therefore be used both to independently define functionally selective fROIs and when residualized, can estimate responses in fROIs for other domains, thereby obviating the need for additional fMRI experiments if additional scans are not possible.

We further asked whether these predictions captured known functional characteristics of each domain, specifically hemispheric laterality. Prediction accuracy reflected the expected lateralization patterns, with substantially higher accuracy for left-hemisphere language fROIs compared to those in the right-hemisphere (Paired t-test, t(34) = 4.78, $p < 0.001$)(Fig. 5), whereas no hemispheric differences were observed for visual and SWM fROIs. Because connectivity estimates were restricted to ipsilateral parcels, the present analyses specifically assess the extent to which within-hemisphere connectivity structure predicts functional selectivity. This restriction may provide a conservative estimate of prediction performance, as contralateral connectivity patterns could also contribute meaningful information, particularly for bilateral systems. Nevertheless, the observed left-lateralized advantage in language prediction is broadly consistent with the stronger and more reliable functional specialization of language cortex in the left hemisphere (Tzourio-Mazoyer et al., 2017). Right-hemisphere language responses are typically weaker and less spatially consistent across individuals (Bavelier et al., 1998; Tzourio-Mazoyer et al., 2017; Vigneau et al., 2011), which may reduce the stability of both the task-evoked responses and their associated connectivity fingerprints (see Joliot et al., 2016; Liu et al., 2009; McAvoy et al., 2016; Wang et al., 2014), thereby lowering prediction accuracy.

3.4. Task-derived connectivity fingerprints are highly similar to resting-state fingerprints

Our connectivity fingerprint models use vertex-to-region correlation matrices of fMRI time series to predict task selectivity. To understand why the models performed similarly even when the source and applied connectivity were different, we examined the similarity between the

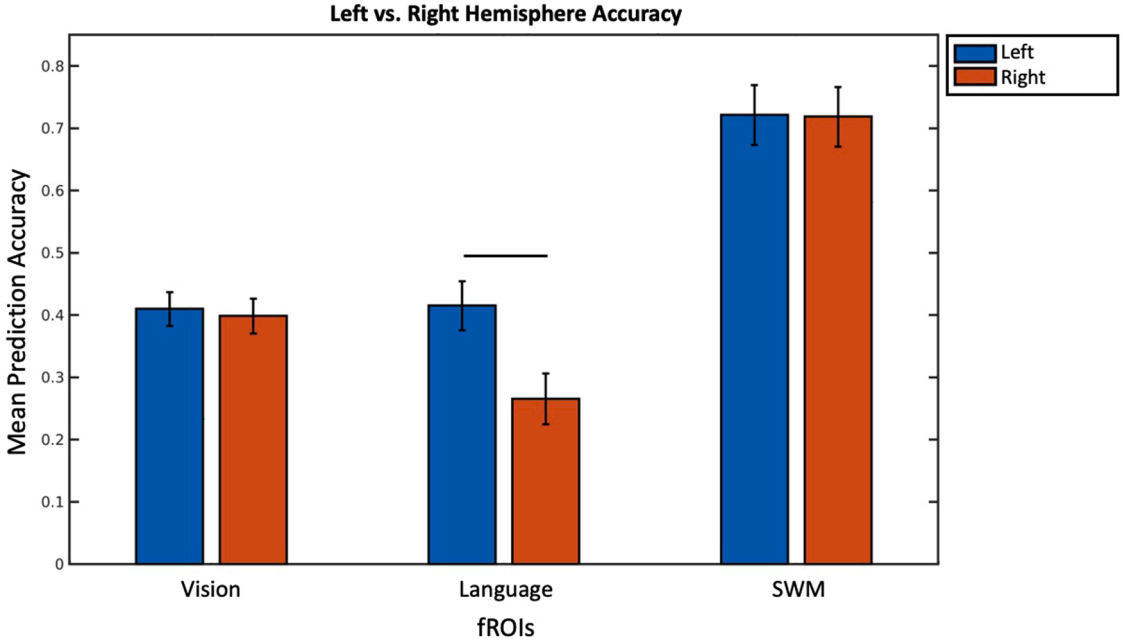

Fig. 5. Comparison of prediction accuracy between left and right fROIs. Bars are grouped by fROI domain. Error bars reflect the standard errors of the means. There is no significant difference at Bonferroni-Holm $p < 0.05$ between left and right visual and SWM fROIs. However, the prediction accuracy for language fROIs is significantly left-lateralized.

patterns of connectivity derived from resting-state and task data by computing the correlations between the resting-state connectivity matrix and the three task-derived connectivity matrices, for each fROI and each participant. We observed that the mean correlations between resting-state and task-derived FC are high ($r > 0.6$) for all three tasks (Fig. 6). Interestingly, FC derived from the auditory language localizer has a significantly higher correlation with resting-state FC than FC derived from the dynamic visual localizer (Paired *t*-test, $t(34) = 3.27$, $p = 0.0025$) and the spatial working memory task (Paired *t*-test, $t(34) = 5.12$, $p < 0.001$). Nevertheless, all three tasks produce patterns of FC that are extremely similar to resting-state FC. And while the connectivity patterns are highly similar (e.g. see Bolt et al., 2017), the data sources might be different at the network level (Bolt et al., 2017). Nonetheless, the predictive connections from these connectivity fingerprinting models are stable enough to mix between different source and applied connectivity type. Thus, the most parsimonious explanation for the above results is that FC is sufficiently similar during rest and specific tasks, such that models can be designed from any FC type, and applied to any FC type as well.

4. Discussion

Here, we show that neural selectivity of an individual can be robustly predicted by task-based connectivity across multiple ROIs associated with a variety of task domains (similar result was found for non-residualized FC; see Supplementary Fig. S2). Our results confirm that FC from one task can be generalized to predict functional activation evoked by other distinct tasks in a variety of functional regions across multiple cortical systems (Figs. 1 and 3). Application of the models to out-of-sample data show high prediction accuracies, providing evidence against overfitting (Fig. 2). Importantly, resting-state FC has no significant advantage in predicting task selectivity over task-derived FC; task data, across our three distinct tasks, can be used to build or be applied by connectivity fingerprint models. Given the well-documented similarity between task FC and resting-state FC (Cho et al., 2021; Elliott et al., 2019; Fair et al., 2007; Gratton et al., 2018b; Kraus et al., 2021), this equivalence in prediction performance is not entirely unexpected, and suggests that task FC preserves enough of the same stable, subject-specific information to be practically substitutable to rest. Still, rest and task FC share about ~35–50% variance, yet models generalized across FC types with equivalent accuracy, indicating the models capture a fingerprint that is stable across meaningfully distinct connectivity estimates. Thus, while previous studies have shown that resting-state FC can be used to predict brain responses at the level of individual subject (e.g., Cole et al., 2016; Ngo et al., 2022; Tavor et al., 2016; Zheng et al., 2022), we extend these findings both to task-derived FC and to an fROI-based approach that offers higher precision and fine-grained information.

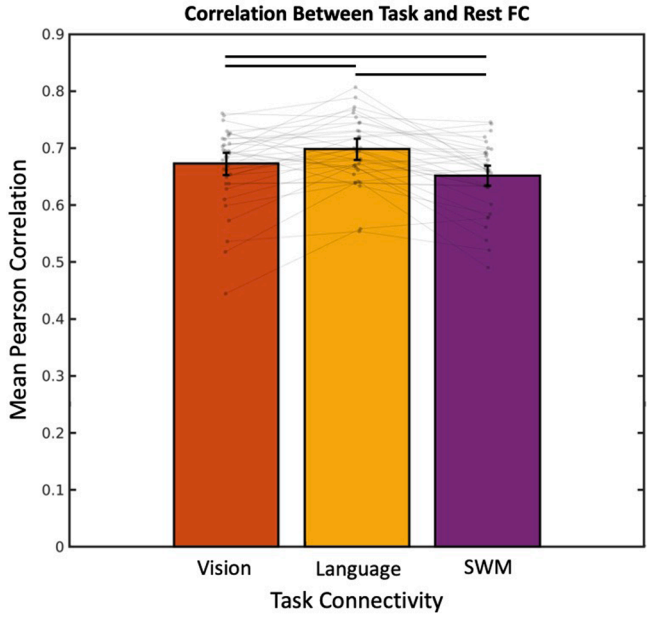

Fig. 6. Correlation between resting-state and task-based connectivity. Each bar represents the overall mean correlation between resting-state and task-derived FC within individual and fROI. Correlations were computed between an individual's rest and task-derived FC matrices. The correlation coefficients were then averaged across fROIs and across subjects. Error bars reflect the standard errors of the means. The significance line indicates a significant difference ($p < 0.05$) between the group means. All three types of task-derived FC are highly similar with resting-state connectivity.

In addition, we demonstrated for the first time that auditory language and multiple-demand (MD) fROIs involved in spatial working memory can be robustly predicted from other task-derived connectivity within individual subjects. These domain-general and domain-specific individual subject fROIs are traditionally defined with functional localizers (e.g., Fedorenko et al., 2010, 2013; Julian et al., 2012). Here we linked functional organization with task-based connectivity, showing that functional connectivity patterns, derived from either resting-state or task data, predicted language-selective and multiple-demand regions at the individual level comparably well (Fig. 2). Notably, MD regions were better predicted than visual and language regions. One possible explanation is that frontoparietal FC carries a richer individual difference signal that is more strongly coupled to cognitive function and more variable across individuals (see Finn et al., 2015b); sensory and language responses, by contrast, may be more strongly driven by feedforward inputs constrained by local circuit organization, which may be less well captured by whole-brain FC. This interpretation is consistent with recent work emphasizing that prefrontal control regions are not isolated executive nodes, but are instead embedded within selectively connected dorsal and ventral attentional-control architectures, with distinct prefrontal subregions showing systematically different connectivity depending on their role in spatial versus non-spatial attention and working memory (Bedini et al., 2023, 2026; Bedini and Baldauf, 2021; Soyuhos and Baldauf, 2023). This selective embedding within broader attentional-control networks may make frontoparietal MD regions particularly amenable to prediction from whole-brain connectivity, since their functional identity is primarily defined through their connectivity profile rather than through local circuit properties. However, this interpretation remains speculative, and several alternative explanations cannot be ruled out, including differences in SNR or task contrast strength, differing reliability of the underlying contrasts (e.g., Hard > Easy for MD versus category contrasts for visual and language regions), or differences in alignment with the Glasser parcellation across domains. Nevertheless, our results advances prior work by demonstrating that connectivity not only reflects large-scale network structure but also captures fine-grained functional organization, including left-laterality of language fROIs. This enables task responses to be predicted without additional localizer scans, even for regions involved in higher cognition, such as the language and MD networks.

The present findings have several implications. First, our results show that task data performs comparably to rest in predicting individual's task selectivity. This equivalence has practical value primarily for datasets in which resting-state scans were not collected or are unavailable: task data can serve as a viable alternative for predicting functional responses in such cases, rather than requiring investigators to acquire additional resting-state scans. Second, the same task dataset can be used both to define functionally selective fROIs for the task performed and to estimate fROIs for other mental domains at the individual-subject level, without requiring a separate, dedicated localizer scan for every domain of interest. This dual use of existing task data may reduce the number of additional localizer acquisitions needed

within a single session, particularly in datasets where only limited scan time is available for functional localization. Of course, the accuracy of task contrast estimates depends on the particular fROIs and domains of interest, as evident in the differences in prediction accuracy between visual, language, and spatial working memory domains (Fig. 2). Dedicated localizers may still be necessary if the best estimates of task effects are desired. Nevertheless, task data may be adequately used to define ROIs in the absence of localizers. Consistent with our previous work (Molloy et al., 2024), connectivity-defined fROIs derived from task data are likely to outperform group-level atlas–based approaches, offering a subject-specific alternative when independent localizers are unavailable. Finally, building on these implications, our approach allows researchers to extract information about task responses of interest even in datasets that lack the corresponding task. This capability is particularly valuable for deeply sampled datasets such as the Natural Scenes Dataset (NSD) (Allen et al., 2022), which offers extensive within-subject sampling and high spatial resolution fMRI data. These properties provide the precision required for studying fine-grained functional organization in brain systems, and make it possible to investigate questions—such as language-related responses—even when an explicit language task was not acquired. Similarly, currently available large-scale fMRI datasets (e.g., Gordon et al., 2017; Miller et al., 2016; Van Essen et al., 2013; Volkow et al., 2018) can be reanalyzed to characterize the functional organization and profiles of brain regions and networks that were not directly acquired, expanding the range of questions that can be addressed with existing data without new acquisitions.

Several considerations and avenues for future work should be noted. First, our training sample (N = 35) is more modest than some recent studies that have demonstrated highly generalizable task prediction from large-scale datasets (e.g., Gal, Tik, et al., 2022; Serin et al., 2025; Tik et al., 2023). We view this as reflecting a distinct and complementary strength of the current approach rather than a limitation. Large-scale datasets offer clear advantages, including broader demographic generalizability and greater statistical power for detecting smaller effect sizes. Nevertheless, connectivity fingerprinting methods have previously been shown to yield robust individual-level predictions with samples considerably smaller than ours—for example, Osher et al. (2019) demonstrated reliable prediction of dorsal attention network organization with as few as nine subjects. Our results extend this previous finding, suggesting that connectivity fingerprint models can achieve meaningful predictive power at sample sizes attainable by individual laboratories, without requiring access to large-scale, multi-site consortium data. Given that many research groups lack the resources to collect datasets on the scale of the Human Connectome Project or similar large public repositories, demonstrating that this approach generalizes well at a more modest, individual-lab-scale sample size broadens its practical accessibility and reproducibility for the wider research community. Another potential concern is cross-task scan parameters. Future studies should test whether predictions extend across distinct tasks and examine how specific fMRI sequence parameters may influence the robustness of predictions (or whether findings generalize across acquisition protocols). One scan parameter that we were concerned about was the variable length of each task; we directly tested this by running all of the analyses with 200 random TRs from each task and rest, and observed very similar results (Supplementary Figure S3). Another question is how task data, with and without residualization (see Supplementary Figure S2), compared to resting-state data, and under what circumstances one may offer advantages over the other. It has been proposed that task engagement may reduce head motion and help maintain arousal, improving data quality over resting-state paradigms. Future work should systematically evaluate these factors to establish the relative strengths, limitations, and optimal applications of task-based vs. resting-state connectivity for studying functional organization and response of brain networks.

Our findings connect to a broader recent literature demonstrating that connectivity fingerprints carry cognitively meaningful information beyond localizing task-evoked responses, including predicting individual differences in perceptual behavior (Soyuhos et al., 2026) and decoding the content of internally generated mental states (Mantegna et al., 2025). Because we show that task-based connectivity captures the similar individual-difference structure as resting-state connectivity for predicting task selectivity, our results suggest that task data may likewise serve as a viable substrate for these richer, behaviorally- and cognitively-relevant applications of connectivity fingerprinting, rather than being limited to localizing functional responses alone.

Our study advances individual-level brain mapping by demonstrating that task-based functional connectivity predicts task activations in high-level visual, language, and spatial working memory regions comparably to resting-state FC. Task-based FC can capture fine-grained individual differences in functional organization, and this predictive power generalizes across domains: connectivity from one task reliably predicted selectivity for domains that task did not directly probe. These findings carry practical implications for large-scale fMRI datasets: where dedicated resting-state or localizer scans are unavailable, existing task data may offer a viable means of inferring individual functional organization, even for domains outside the scope of the task performed. This underscores the value of individual FC fingerprints, derived from either task or rest, for characterizing the brain's functional architecture.

Ethics statement

All experimental procedures were approved by the Institutional Review Board of The Ohio State University. Written informed consent was obtained from all participants prior to participation, in accordance with the Declaration of Helsinki.

Funding

Funding was generously provided by the Alfred P Sloan Foundation (Z.M.S.), the College of Arts and Sciences, The Ohio State University, and the Chronic Brain Injury Program, The Ohio State University.

CRediT authorship contribution statement

Isaac Liao: Writing – review & editing, Writing – original draft, Visualization, Investigation, Formal analysis. **Zeynep M. Saygin:** Writing – review & editing, Funding acquisition, Formal analysis, Data curation. **Keara M. Ginell:** Writing – review & editing. **Kendrick N. Kay:** Writing – review & editing, Conceptualization. **David E. Osher:** Writing – review & editing, Visualization, Methodology, Investigation, Funding acquisition, Formal analysis, Conceptualization.

Declaration of competing interest

The authors declare that they have no known competing financial interests or personal relationships that could have appeared to influence the work reported in this paper.

Supplementary materials

Supplementary material associated with this article can be found, in the online version, at doi:10.1016/j.neuroimage.2026.122211.

Data availability

Data and code are available upon request.

References

Allen, E.J., St-Yves, G., Wu, Y., Breedlove, J.L., Prince, J.S., Dowdle, L.T., Nau, M., Caron, B., Pestilli, F., Charest, I., Hutchinson, J.B., Naselaris, T., Kay, K., 2022. A massive 7T fMRI dataset to bridge cognitive neuroscience and artificial

intelligence. Nat. Neurosci. 25 (1), 116–126. https://doi.org/10.1038/s41593-021-00962-x.
Bavelier, D., Corina, D., Jezzard, P., Clark, V., Karni, A., Lalwani, A., Rauschecker, J.P., Braun, A., Turner, R., Neville, H.J., 1998. Hemispheric specialization for English and ASL: left invariance-right variability. Neuroreport 9 (7), 1537–1542.
Bedini, M., Baldauf, D., 2021. Structure, function and connectivity fingerprints of the frontal eye field versus the inferior frontal junction: a comprehensive comparison. Eur. J. Neurosci. 54 (4), 5462–5506. https://doi.org/10.1111/ejn.15393.
Bedini, M., Olivetti, E., Avesani, P., Baldauf, D., 2023. Accurate localization and coactivation profiles of the frontal eye field and inferior frontal junction: an ALE and MACM fMRI meta-analysis. Brain Struct. Funct. 228 (3), 997–1017. https://doi.org/10.1007/s00429-023-02641-y.
Bedini, M., Olivetti, E., Avesani, P., Baldauf, D., 2026. Surface-based tractography uncovers 'what' and 'where' pathways in prefrontal cortex. Cortex 199, 129–144. https://doi.org/10.1016/j.cortex.2026.03.016.
Behzadi, Y., Restom, K., Liau, J., Liu, T.T., 2007. A component based noise correction method (CompCor) for BOLD and perfusion based fMRI. Neuroimage 37 (1), 90–101. https://doi.org/10.1016/j.neuroimage.2007.04.042.
Bernstein-Eliav, M., Tavor, I., 2024. The prediction of brain activity from connectivity: advances and applications. Neuroscientist 30 (3), 367–377. https://doi.org/10.1177/10738584221130974.
Biswal, B., Zerrin Yetkin, F., Haughton, V.M., Hyde, J.S., 1995. Functional connectivity in the motor cortex of resting human brain using echo-planar mri. Magn. Reson. Med. 34 (4), 537–541. https://doi.org/10.1002/mrm.1910340409.
Bolt, T., Nomi, J.S., Rubinov, M., Uddin, L.Q., 2017. Correspondence between evoked and intrinsic functional brain network configurations. Hum. Brain Mapp. 38 (4), 1992–2007. https://doi.org/10.1002/hbm.23500.
Buckner, R.L., Krienen, F.M., Yeo, B.T.T., 2013. Opportunities and limitations of intrinsic functional connectivity MRI. Nat. Neurosci. 16 (7), 832–837. https://doi.org/10.1038/nn.3423.
Cho, J.W., Korchmaros, A., Vogelstein, J.T., Milham, M.P., Xu, T., 2021. Impact of concatenating fMRI data on reliability for functional connectomics. Neuroimage 226, 117549. https://doi.org/10.1016/j.neuroimage.2020.117549.
Cole, M.W., Ito, T., Bassett, D.S., Schultz, D.H., 2016. Activity flow over resting-state networks shapes cognitive task activations. Nat. Neurosci. 19 (12), 1718–1726. https://doi.org/10.1038/nn.4406.
Dale, A.M., Fischl, B., Sereno, M.I., 1999. Cortical surface-based analysis: I. Segmentation and surface reconstruction. Neuroimage 9 (2), 179–194. https://doi.org/10.1006/nimg.1998.0395.
DiNicola, L.M., Braga, R.M., Buckner, R.L., 2020. Parallel distributed networks dissociate episodic and social functions within the individual. J. Neurophysiol. 123 (3), 1144–1179. https://doi.org/10.1152/jn.00529.2019.
Dosenbach, N.U.F., Fair, D.A., Miezin, F.M., Cohen, A.L., Wenger, K.K., Dosenbach, R.A. T., Fox, M.D., Snyder, A.Z., Vincent, J.L., Raichle, M.E., Schlaggar, B.L., Petersen, S. E., 2007. Distinct brain networks for adaptive and stable task control in humans. Proc. Natl. Acad. Sci. 104 (26), 11073–11078. https://doi.org/10.1073/pnas.0704320104.
Dosenbach, N.U.F., Nardos, B., Cohen, A.L., Fair, D.A., Power, J.D., Church, J.A., Nelson, S.M., Wig, G.S., Vogel, A.C., Lessov-Schlaggar, C.N., Barnes, K.A., Dubis, J. W., Feczko, E., Coalson, R.S., Pruett, J.R., Barch, D.M., Petersen, S.E., Schlaggar, B. L., 2010. Prediction of individual brain maturity using fMRI. Science 329 (5997), 1358–1361. https://doi.org/10.1126/science.1194144.
Du, J., Tripathi, V., Elliott, M.L., Ladopoulou, J., Sun, W., Eldaief, M.C., Buckner, R.L., 2025. Within-individual precision mapping of brain networks exclusively using task data. Neuron 113, 4069–4083.e6. https://doi.org/10.1016/j.neuron.2025.08.029.
Dubois, J., Galdi, P., Han, Y., Paul, L.K., Adolphs, R., 2018. Resting-State functional brain connectivity best predicts the personality dimension of openness to experience. Personal. Neurosci. 1, e6. https://doi.org/10.1017/pen.2018.8.
Elliott, M.L., Knodt, A.R., Cooke, M., Kim, M.J., Melzer, T.R., Keenan, R., Ireland, D., Ramrakha, S., Poulton, R., Caspi, A., Moffitt, T.E., Hariri, A.R., 2019. General functional connectivity: shared features of resting-state and task fMRI drive reliable and heritable individual differences in functional brain networks. Neuroimage 189, 516–532. https://doi.org/10.1016/j.neuroimage.2019.01.068.
Fair, D.A., Schlaggar, B.L., Cohen, A.L., Miezin, F.M., Dosenbach, N.U.F., Wenger, K.K., Fox, M.D., Snyder, A.Z., Raichle, M.E., Petersen, S.E., 2007. A method for using blocked and event-related fMRI data to study "resting state" functional connectivity. Neuroimage 35 (1), 396–405. https://doi.org/10.1016/j.neuroimage.2006.11.051.
Farràs-Permanyer, L., Mancho-Fora, N., Montalà-Flaquer, M., Bartrés-Faz, D., Vaqué-Alcázar, L., Peró-Cebollero, M., Guàrdia-Olmos, J., 2019. Age-related changes in resting-state functional connectivity in older adults. Neural Regen. Res. 14 (9), 1544–1555. https://doi.org/10.4103/1673-5374.255976.
Fedorenko, E., Duncan, J., Kanwisher, N., 2013. Broad domain generality in focal regions of frontal and parietal cortex. Proc. Natl. Acad. Sci. 110 (41), 16616–16621. https://doi.org/10.1073/pnas.1315235110.
Fedorenko, E., Hsieh, P.-J., Nieto-Castañón, A., Whitfield-Gabrieli, S., Kanwisher, N., 2010. New method for fMRI investigations of language: defining ROIs functionally in individual subjects. J. Neurophysiol. 104 (2), 1177–1194. https://doi.org/10.1152/jn.00032.2010.
Finn, E.S., 2021. Is it time to put rest to rest? Trends Cogn. Sci. (Regul. Ed.) 25 (12), 1021–1032. https://doi.org/10.1016/j.tics.2021.09.005.
Finn, E.S., Bandettini, P.A., 2021. Movie-watching outperforms rest for functional connectivity-based prediction of behavior. Neuroimage 235, 117963. https://doi.org/10.1016/j.neuroimage.2021.117963.
Finn, E.S., Shen, X., Scheinost, D., Rosenberg, M.D., Huang, J., Chun, M.M., Papademetris, X., Constable, R.T., 2015a. Functional connectome fingerprinting: identifying individuals using patterns of brain connectivity. Nat. Neurosci. 18 (11), 1664–1671. https://doi.org/10.1038/nn.4135.
Finn, E.S., Shen, X., Scheinost, D., Rosenberg, M.D., Huang, J., Chun, M.M., Papademetris, X., Constable, R.T., 2015b. Functional connectome fingerprinting: identifying individuals using patterns of brain connectivity. Nat. Neurosci. 18 (11), 1664–1671. https://doi.org/10.1038/nn.4135.
Fischl, B., 2012. FreeSurfer. NeuroImage 20 Years fMRI 62 (2), 774–781. https://doi.org/10.1016/j.neuroimage.2012.01.021.
Fox, M.D., Raichle, M.E., 2007. Spontaneous fluctuations in brain activity observed with functional magnetic resonance imaging. Nat. Rev. Neurosci. 8 (9), 700–711. https://doi.org/10.1038/nrn2201.
Gal, S., Coldham, Y., Tik, N., Bernstein-Eliav, M., Tavor, I., 2022a. Act natural: functional connectivity from naturalistic stimuli fMRI outperforms resting-state in predicting brain activity. Neuroimage 258, 119359. https://doi.org/10.1016/j.neuroimage.2022.119359.
Geerligs, L., Rubinov, M., Cam-CAN, Henson, R.N, 2015. State and trait components of functional connectivity: individual differences vary with mental State. J. Neurosci. 35 (41), 13949–13961. https://doi.org/10.1523/JNEUROSCI.1324-15.2015.
Gordon, E.M., Laumann, T.O., Gilmore, A.W., Newbold, D.J., Greene, D.J., Berg, J.J., Ortega, M., Hoyt-Drazen, C., Gratton, C., Sun, H., Hampton, J.M., Coalson, R.S., Nguyen, A.L., McDermott, K.B., Shimony, J.S., Snyder, A.Z., Schlaggar, B.L., Petersen, S.E., Nelson, S.M., Dosenbach, N.U.F., 2017. Precision functional mapping of individual Human brains. Neuron 95 (4), 791–807.e7. https://doi.org/10.1016/j.neuron.2017.07.011.
Gratton, C., Laumann, T.O., Nielsen, A.N., Greene, D.J., Gordon, E.M., Gilmore, A.W., Nelson, S.M., Coalson, R.S., Snyder, A.Z., Schlaggar, B.L., Dosenbach, N.U.F., Petersen, S.E., 2018a. Functional brain networks are dominated by stable group and individual factors, not cognitive or daily variation. Neuron 98 (2), 439–452.e5. https://doi.org/10.1016/j.neuron.2018.03.035.
Gratton, C., Laumann, T.O., Nielsen, A.N., Greene, D.J., Gordon, E.M., Gilmore, A.W., Nelson, S.M., Coalson, R.S., Snyder, A.Z., Schlaggar, B.L., Dosenbach, N.U.F., Petersen, S.E., 2018b. Functional brain networks are dominated by stable group and individual factors, not cognitive or daily variation. Neuron 98 (2), 439–452.e5. https://doi.org/10.1016/j.neuron.2018.03.035.
Greene, A.S., Gao, S., Noble, S., Scheinost, D., Constable, R.T., 2020. How tasks change whole-brain functional organization to reveal brain-phenotype relationships. Cell Rep. 32 (8), 108066. https://doi.org/10.1016/j.celrep.2020.108066.
Greene, A.S., Gao, S., Scheinost, D., Constable, R.T., 2018. Task-induced brain state manipulation improves prediction of individual traits. Nat. Commun. 9 (1), 2807. https://doi.org/10.1038/s41467-018-04920-3.
Hiersche, K.J., Saygin, Z.M., Osher, D.E., 2025. Connectivity and function are coupled across cognitive domains throughout the brain, 2025.07.09.663763 bioRxiv. https://doi.org/10.1101/2025.07.09.663763.
Hsu, W.-T., Rosenberg, M.D., Scheinost, D., Constable, R.T., Chun, M.M., 2018. Resting-state functional connectivity predicts neuroticism and extraversion in novel individuals. Soc. Cogn. Affect. Neurosci. 13 (2), 224–232. https://doi.org/10.1093/scan/nsy002.
Hua, L., Gao, F., Xia, X., Guo, Q., Zhao, Y., Huang, S., Yuan, Z., 2023. Individual-specific functional connectivity improves prediction of Alzheimer's disease's symptoms in elderly people regardless of APOE ε4 genotype. Commun. Biol. 6 (1), 581. https://doi.org/10.1038/s42003-023-04952-6.
Jiang, R., Zuo, N., Ford, J.M., Qi, S., Zhi, D., Zhuo, C., Xu, Y., Fu, Z., Bustillo, J., Turner, J.A., Calhoun, V.D., Sui, J., 2020. Task-induced brain connectivity promotes the detection of individual differences in brain-behavior relationships. Neuroimage 207, 116370. https://doi.org/10.1016/j.neuroimage.2019.116370.
Joliot, M., Tzourio-Mazoyer, N., Mazoyer, B., 2016. Intra-hemispheric intrinsic connectivity asymmetry and its relationships with handedness and language lateralization. Neuropsychol. Neural Bases Hemispheric Spec. 93, 437–447. https://doi.org/10.1016/j.neuropsychologia.2016.03.013.
Julian, J.B., Fedorenko, E., Webster, J., Kanwisher, N., 2012. An algorithmic method for functionally defining regions of interest in the ventral visual pathway. Neuroimage 60 (4), 2357–2364. https://doi.org/10.1016/j.neuroimage.2012.02.055.
Kelly, A.M.C., Uddin, L.Q., Biswal, B.B., Castellanos, F.X., Milham, M.P., 2008. Competition between functional brain networks mediates behavioral variability. Neuroimage 39 (1), 527–537. https://doi.org/10.1016/j.neuroimage.2007.08.008.
Kraus, B.T., Perez, D., Ladwig, Z., Seitzman, B.A., Dworetsky, A., Petersen, S.E., Gratton, C., 2021. Network variants are similar between task and rest states. Neuroimage 229, 117743. https://doi.org/10.1016/j.neuroimage.2021.117743.
Lake, E.M.R., Finn, E.S., Noble, S.M., Vanderwal, T., Shen, X., Rosenberg, M.D., Spann, M.N., Chun, M.M., Scheinost, D., Constable, R.T., 2019. The functional brain organization of an individual allows prediction of measures of social abilities transdiagnostically in autism and attention-deficit/hyperactivity disorder. Biol. Psychiatry Autism Spectr. Disord.: Mech. Features 86 (4), 315–326. https://doi.org/10.1016/j.biopsych.2019.02.019.
Li, J., Osher, D.E., Hansen, H.A., Saygin, Z.M., 2020. Innate connectivity patterns drive the development of the visual word form area. Sci. Rep. 10 (1), 18039. https://doi.org/10.1038/s41598-020-75015-7.
Liu, H., Stufflebeam, S.M., Sepulcre, J., Hedden, T., Buckner, R.L., 2009. Evidence from intrinsic activity that asymmetry of the human brain is controlled by multiple factors. Proc. Natl. Acad. Sci. 106 (48), 20499–20503. https://doi.org/10.1073/pnas.0908073106.
Mahon, B.Z., Caramazza, A., 2011. What drives the organization of object knowledge in the brain? Trends Cogn. Sci. (Regul. Ed.) 15 (3), 97–103. https://doi.org/10.1016/j.tics.2011.01.004.
Mantegna, F., Olivetti, E., Schwedhelm, P., Baldauf, D., 2025. Covariance-based decoding reveals a category-specific functional connectivity network for imagined

visual objects. Neuroimage 311, 121171. https://doi.org/10.1016/j.neuroimage.2025.121171.
Mars, R.B., Passingham, R.E., Jbabdi, S., 2018. Connectivity fingerprints: from areal descriptions to abstract spaces. Trends Cogn. Sci. (Regul. Ed.) 22 (11), 1026–1037. https://doi.org/10.1016/j.tics.2018.08.009.
McAvoy, M., Mitra, A., Coalson, R.S., d'Avossa, G., Keidel, J.L., Petersen, S.E., Raichle, M.E., 2016. Unmasking language lateralization in Human brain intrinsic activity. Cereb. Cortex 26 (4), 1733–1746. https://doi.org/10.1093/cercor/bhv007.
Miller, K.L., Alfaro-Almagro, F., Bangerter, N.K., Thomas, D.L., Yacoub, E., Xu, J., Bartsch, A.J., Jbabdi, S., Sotiropoulos, S.N., Andersson, J.L.R., Griffanti, L., Douaud, G., Okell, T.W., Weale, P., Dragonu, I., Garratt, S., Hudson, S., Collins, R., Jenkinson, M., Smith, S.M., 2016. Multimodal population brain imaging in the UK Biobank prospective epidemiological study. Nat. Neurosci. 19 (11), 1523–1536. https://doi.org/10.1038/nn.4393.
Molloy, M.F., Saygin, Z.M., Osher, D.E., 2024. Predicting high-level visual areas in the absence of task fMRI. Sci. Rep. 14 (1), 11376. https://doi.org/10.1038/s41598-024-62098-9.
Morcom, A.M., Fletcher, P.C., 2007. Does the brain have a baseline? Why we should be resisting a rest. Neuroimage 37 (4), 1073–1082. https://doi.org/10.1016/j.neuroimage.2006.09.013.
Ngo, G.H., Khosla, M., Jamison, K., Kuceyeski, A., Sabuncu, M.R., 2022. Predicting individual task contrasts from resting-state functional connectivity using a surface-based convolutional network. Neuroimage 248, 118849. https://doi.org/10.1016/j.neuroimage.2021.118849.
Nielsen, A.N., Greene, D.J., Gratton, C., Dosenbach, N.U.F., Petersen, S.E., Schlaggar, B.L., 2019. Evaluating the prediction of brain maturity from functional connectivity after motion artifact denoising. Cereb. Cortex (N. Y. NY) 29 (6), 2455–2469. https://doi.org/10.1093/cercor/bhy117.
Osher, D.E., Brissenden, J.A., Somers, D.C., 2019. Predicting an individual's dorsal attention network activity from functional connectivity fingerprints. J. Neurophysiol. 122 (1), 232–240. https://doi.org/10.1152/jn.00174.2019.
Osher, D.E., Saxe, R.R., Koldewyn, K., Gabrieli, J.D.E., Kanwisher, N., Saygin, Z.M., 2016. Structural connectivity fingerprints predict cortical selectivity for multiple visual categories across cortex. Cereb. Cortex 26 (4), 1668–1683. https://doi.org/10.1093/cercor/bhu303.
Parker Jones, O., Voets, N.L., Adcock, J.E., Stacey, R., Jbabdi, S., 2017. Resting connectivity predicts task activation in pre-surgical populations. NeuroImage : Clin. 13, 378–385. https://doi.org/10.1016/j.nicl.2016.12.028.
Passingham, R.E., Stephan, K.E., Kötter, R., 2002. The anatomical basis of functional localization in the cortex. Nat. Rev. Neurosci. 3 (8), 606–616. https://doi.org/10.1038/nrn893.
Ratan Murty, N.A., Teng, S., Beeler, D., Mynick, A., Oliva, A., Kanwisher, N., 2020. Visual experience is not necessary for the development of face-selectivity in the lateral fusiform gyrus. Proc. Natl. Acad. Sci. 117 (37), 23011–23020. https://doi.org/10.1073/pnas.2004607117.
Salehi, M., Greene, A.S., Karbasi, A., Shen, X., Scheinost, D., Constable, R.T., 2020. There is no single functional atlas even for a single individual: functional parcel definitions change with task. Neuroimage 208, 116366. https://doi.org/10.1016/j.neuroimage.2019.116366.
Saygin, Z.M., Osher, D.E., Koldewyn, K., Reynolds, G., Gabrieli, J.D.E., Saxe, R.R., 2012. Anatomical connectivity patterns predict face selectivity in the fusiform gyrus. Nat. Neurosci. 15 (2), 321–327. https://doi.org/10.1038/nn.3001.
Serin, E., Ritter, K., Schumann, G., Banaschewski, T., Marquand, A., Walter, H., 2025. Generating synthetic task-based brain fingerprints for population neuroscience using deep learning. Commun. Biol. 8 (1), 1572. https://doi.org/10.1038/s42003-025-09158-6.
Smith, S.M., Nichols, T.E., Vidaurre, D., Winkler, A.M., Behrens, T.E.J., Glasser, M.F., Ugurbil, K., Barch, D.M., Van Essen, D.C., Miller, K.L., 2015. A positive-negative mode of population covariation links brain connectivity, demographics and behavior. Nat. Neurosci. 18 (11), 1565–1567. https://doi.org/10.1038/nn.4125.
Song, H., Rosenberg, M.D., 2021. Predicting attention across time and contexts with functional brain connectivity. *Current Opinion in Behavioral Sciences*. Deep Imaging - Pers. Neurosci. 40, 33–44. https://doi.org/10.1016/j.cobeha.2020.12.007.
Soyuhos, O., Baldauf, D., 2023. Functional connectivity fingerprints of the frontal eye field and inferior frontal junction suggest spatial versus nonspatial processing in the prefrontal cortex. Eur. J. Neurosci. 57 (7), 1114–1140. https://doi.org/10.1111/ejn.15936.
Soyuhos, O., Scarpa, A., Baldauf, D., 2026. Distinct resting-State connectomes for face and scene perception predict individual task performance. Hum. Brain Mapp. 47 (5), e70498. https://doi.org/10.1002/hbm.70498.
Sripada, C., Angstadt, M., Rutherford, S., Taxali, A., Shedden, K., 2020. Toward a "treadmill test" for cognition: improved prediction of general cognitive ability from the task activated brain. Hum. Brain Mapp. 41 (12), 3186–3197. https://doi.org/10.1002/hbm.25007.
Tavor, I., Jones, O.P., Mars, R.B., Smith, S.M., Behrens, T.E., Jbabdi, S., 2016. Task-free MRI predicts individual differences in brain activity during task performance. Science 352 (6282), 216–220. https://doi.org/10.1126/science.aad8127.
Tik, N., Gal, S., Madar, A., Ben-David, T., Bernstein-Eliav, M., Tavor, I., 2023. Generalizing prediction of task-evoked brain activity across datasets and populations. Neuroimage 276, 120213. https://doi.org/10.1016/j.neuroimage.2023.120213.
Tik, N., Livny, A., Gal, S., Gigi, K., Tsarfaty, G., Weiser, M., Tavor, I., 2021. Predicting individual variability in task-evoked brain activity in schizophrenia. Hum. Brain Mapp. 42 (12), 3983–3992. https://doi.org/10.1002/hbm.25534.
Tobyne, S.M., Somers, D.C., Brissenden, J.A., Michalka, S.W., Noyce, A.L., Osher, D.E., 2018. Prediction of individualized task activation in sensory modality-selective frontal cortex with 'connectome fingerprinting'. Neuroimage 183, 173–185. https://doi.org/10.1016/j.neuroimage.2018.08.007.
Tzourio-Mazoyer, N., Perrone-Bertolotti, M., Jobard, G., Mazoyer, B., Baciu, M., 2017. Multi-factorial modulation of hemispheric specialization and plasticity for language in healthy and pathological conditions: a review. Cortex Is "Single" Brain Model Sufficient? 86, 314–339. https://doi.org/10.1016/j.cortex.2016.05.013.
Van Essen, D.C., Smith, S.M., Barch, D.M., Behrens, T.E.J., Yacoub, E., Ugurbil, K., 2013. The WU-minn human connectome project: an overview. NeuroImage Mapp. Connect. 80, 62–79. https://doi.org/10.1016/j.neuroimage.2013.05.041.
Vigneau, M., Beaucousin, V., Hervé, P.-Y., Jobard, G., Petit, L., Crivello, F., Mellet, E., Zago, L., Mazoyer, B., Tzourio-Mazoyer, N., 2011. What is right-hemisphere contribution to phonological, lexico-semantic, and sentence processing?: insights from a meta-analysis. Neuroimage 54 (1), 577–593. https://doi.org/10.1016/j.neuroimage.2010.07.036.
Volkow, N.D., Koob, G.F., Croyle, R.T., Bianchi, D.W., Gordon, J.A., Koroshetz, W.J., Pérez-Stable, E.J., Riley, W.T., Bloch, M.H., Conway, K., Deeds, B.G., Dowling, G.J., Grant, S., Howlett, K.D., Matochik, J.A., Morgan, G.D., Murray, M.M., Noronha, A., Spong, C.Y., Weiss, S.R.B, 2018. The conception of the ABCD study: from substance use to a broad NIH collaboration. Dev. Cogn. Neurosci. Adolesc. Brain Cogn. Dev. (ABCD) Consort.: Ration. Aims Assess. Strategy 32, 4–7. https://doi.org/10.1016/j.dcn.2017.10.002.
Wang, D., Buckner, R.L., Liu, H., 2014. Functional specialization in the Human brain estimated by intrinsic hemispheric interaction. J. Neurosci. 34 (37), 12341–12352. https://doi.org/10.1523/JNEUROSCI.0787-14.2014.
Wei, W., Zhang, K., Chang, J., Zhang, S., Ma, L., Wang, H., Zhang, M., Zu, Z., Yang, L., Chen, F., Fan, C., Li, X., 2024. Analyzing 20 years of resting-State fMRI research: trends and collaborative networks revealed. Brain Res. 1822, 148634. https://doi.org/10.1016/j.brainres.2023.148634.
Yin, W., Li, T., Wu, Z., Hung, S.-C., Hu, D., Gui, Y., Cho, S., Sun, Y., Woodburn, M.A., Wang, L., Li, G., Piven, J., Elison, J.T., Wu, C.W., Zhu, H., Cohen, J.R., Lin, W., 2025. Charting brain functional development from birth to 6 years of age. Nat. Hum. Behav. 9 (6), 1246–1259. https://doi.org/10.1038/s41562-025-02160-2.
Zheng, Y.-Q., Farahibozorg, S.-R., Gong, W., Rafipoor, H., Jbabdi, S., Smith, S., 2022. Accurate predictions of individual differences in task-evoked brain activity from resting-state fMRI using a sparse ensemble learner. Neuroimage 259, 119418. https://doi.org/10.1016/j.neuroimage.2022.119418.